

Multi-observatory observations of night-side of Venus at 2.3 micron - atmospheric circulation from tracking of cloud features

Sanjay Limaye^{1*}, Johan Warell², Bhuwan C. Bhatt³, Patrick M. Fry¹,
and Eliot F. Young⁴

¹*Space Science and Engineering Center, University of Wisconsin, Madison, WI 53706, US*

²*Department of Astronomy and Space Physics, Uppsala University, Uppsala, Sweden*

³*Centre for Research and Education in Science and Technology, Indian Institute of Astrophysics, Hosakote, India*

⁴*Southwest Research Institute, Boulder, Colorado, USA*

Received 23 November 2005; accepted 14 March 2006

Abstract. Observations of Venus were made during 3 May to 11 May 2004 (117.4° – 125.7° phase angle) and 3 July to 10 July, 2004 (132.5° – 125.1° phase angle) from the 1.2-metre Mt. Abu Telescope at Gurushikhar, Himalayan Chandra Telescope at Mt. Saraswati, Hanle and the Nordic Optical Telescope at La Palma, Canary Islands and the NASA/Infra Red Telescope Facility (IRTF) at Mauna Kea, Hawaii in J and K bands. While the sunlit crescent portion was saturated in the detector, the night-side shows discrete cloud features. These features are seen to evolve over time and are markers of the atmospheric flow at or below ~53 km altitude above the surface. By combining multi-site observations, we are able to make measurements of zonal cloud velocities over baselines that are several hours long and get a better idea of the evolution of the features over time.

Keywords : Venus night-side; near infrared, atmosphere circulation

*e-mail:SanjayL@ssec.wisc.edu

1. Introduction

The thick cloud cover observed on Venus and its high surface temperature and pressure continue to present challenges for understanding the planet and its atmosphere. Studies of the atmospheric circulation of Venus have relied on tracking of entry probes from the Earth and cloud motions. Atmospheric circulation of Venus has been a puzzle for a long time – it has been observed to be retrograde everywhere on the planet from near surface to the cloud top level (~ 70 km) and higher. Venus exhibits no contrast at visible wavelengths and at thermal infrared wavelengths emission from the cloud cover at ~ 65 km is detectable. Global observations of the Venus circulation have been generally made from spacecraft in reflected ultraviolet-blue region of the spectrum, and hence are restricted to the daylight portion of the planet.

In 1983, narrow “windows” in the near infrared spectrum of Venus between about 1 - 2.5 μm were discovered by Allen and Crawford (1984) that showed that despite the thick cloud cover, thermal emission from the lower atmosphere and the surface can be detected (Allen, 1987). These new windows into the lower Venus atmosphere were exploited for very limited observations during 1990 by the NIMS instrument on the Galileo Orbiter on its roundabout journey to Jupiter (Carlson et al., 1991, 1993; Baines and Carlson, 1991). Subsequently, cloud motions have been determined from groundbased (Bell et al., 1991; Crisp et al., 1991; Meadows and Crisp, 1996; Chanover et al., 1998) and spacecraft (Carlson et al., 1991) observations of Venus during the Galileo spacecraft’s fly-by of Venus on its way to Jupiter. Earth-based observations around the Venus fly-by date also yielded some results from feature tracking in near infrared images of Venus from multiple observatories (Crisp et al., 1991). These observations confirmed that the Venus atmosphere and its thermal structure below the cloud is far from globally uniform and is quite dynamic, changing on a time scale of hours to days and weeks. The spatial contrasts in the near infrared observations are inferred to be due to variation in the optical thickness of the overlying sulfuric acid cloud as well as variation of trace species such as water vapor. The mechanisms for these changes are poorly understood primarily because of insufficient observations.

Radiative transfer analysis has shown that at wavelengths between 1.7–2.5 μm the radiation measured from Venus from outside the atmosphere is primarily being emitted from levels above the 8 bar (30 km) pressure level, whereas at 1.74 μm the radiation is produced at deeper levels (Bell et al., 1991). A substantial spatial variation in the radiation emanating from Venus is seen between 2.21 and 2.32 μm , which produce the light (hot spots or more emission) and dark markings (cooler spots, i.e. less emission) in images used in this study. Between about 2.2 μm and 2.5 μm , H_2SO_4 clouds and CO_2 contribute most towards the extinction with weaker contributions from CO, water vapor and other gases (Bell et al., 1991). Crisp et al. (1989) and Kamp and Taylor (1990) showed that the spatial variability of the observed thermal emission from the dark side of Venus was due to variations in optical depth due to the sulfuric acid clouds and that the height at which the thermal optical depth of this cloud was ~ 48 km at 2.3 μm

(unity thermal optical depth) and extending to as high as ~ 55 km at $2.32 \mu\text{m}$. Thus, with the $\sim 20 - 50$ nm bandpass filters we utilized in the study, the features observed are expected to represent the Venus atmosphere and its motions at ~ 53 km altitude. Obtaining images separated by an interval of ~ 30 min to as much as a few hours provides discrete measurements of the location of the features, the largest of which have been observed for several days. These position measurements on Venus when combined with the times when they are observed provide us with a good estimate of the atmospheric wind at ~ 53 km level. This is supported by the general agreement between the zonal winds measured by entry probes and the drift rates of the near IR features in previous studies (Crisp et al., 1991; Carlson et al., 1991). Further, a lower limit (30 km or 8 bars atmospheric pressure) on the altitude of the $2.3 \mu\text{m}$ emissions is provided by analysis of high resolution spectra by Bezdard et al., (1990). They also show that the $1.74 \mu\text{m}$ emissions come from deeper (warmer) levels of the Venus atmosphere.

Observing Venus with sufficient angular resolution is challenging and use of adaptive optics (AO) is not applicable because it is an extended source (most Astronomical AO systems need a “point” source, so planets such as Neptune or Pluto which are ~ 2.3 arcseconds in diameter or less as seen from Earth are generally the only planets that can be observed with current AO system). Laser guided systems also are not available for Venus because the sky brightness is generally too high and the elevation too low. Thus high quality observations of Venus depend to a large degree on the atmospheric seeing and longevity of the observing period.

The Visible Infrared Thermal Imaging Spectrometer (VIRTIS) instrument on the European Space Agency’s Venus Express mission (Chicarro, 2003; Svedhem et al., 2005) launched in November 2005 will provide temporal and spectroscopic coverage of Venus from orbit after arriving at Venus in April 2006. Images will be obtained in the wavelength range $0.25 - 5 \mu\text{m}$ using two separate detectors - a CCD for $0.25 - 1 \mu\text{m}$, and a Focal Plane Array (FPA) for the $1 - 5 \mu\text{m}$ range. The Earth-based telescopic observations using a filter at $2.3 \mu\text{m}$ thus provide a useful preview of the kind of data that will be gathered from Venus Express and help in planning the observational coverage.

2. Observations

The proximity to the Sun and its intrinsic brightness make Venus a challenging object to observe from large telescopes. Because of the inability in most cases to observe Venus during the daytime at infrared wavelengths and the need to observe Venus near sunset, Venus is accessible to most observatories for a very limited time (~ 2 hours) before its elevation becomes too low. Even when Venus is lit only as a crescent at high phase angles, the reflected solar radiance from the Venus crescent at $1 - 3 \mu\text{m}$ wavelengths is much greater than the emission from the lower atmosphere. Hence a coronagraph is desirable to mask the sunlit crescent, but generally not available at sites for use with NIR detectors. The desired periods (large phase angles) thus conflict with the ability

to observe Venus in terms of its proximity to the Sun. By using observatories spaced in longitude, we can extend the coverage of the Venus atmosphere by using the rotation of the Earth to provide multiple short looks at Venus on the same day. This is essential for monitoring the displacements of the cloud features in the Venus atmosphere, due both to the speed of the features and the relatively low spatial resolution of the observations currently possible from Earth.

The location of the observatories that observed Venus during May 2004 are given in Table 1. The K filter was used at all of the sites for the images. At the NASA Infra Red Telescope Facility (IRTF) in Hawaii, spectra were also acquired using the SPeX instrument (Rayner et al., 2003). The multi-observatory campaign at widely separated longitudes provided Venus observation over \sim two hour each and separated by \sim five and \sim 10 hours between the Nordic Optical Telescope (NOT), Himalayan Chandra Telescope (HCT), Mt. Abu and IRTF. The east to west drift due to the prevailing winds in the Venus atmosphere at altitudes below \sim 53 km is less than \sim 2° longitude per hour in equatorial and mid-latitudes (Kerzhanovich and Limaye, 1983), so that each “day”, one would expect to find a given cloud feature in all three observatory data, unless it drifted off from the visible disk of Venus by the prevailing east-to-west flow.

Table 1. Coordinated observations of night-side of Venus.

Observatory	HCT	MtAbu	NOT	IRTF
Latitude	32° 46' 46" N	24° 39' 8.8" N	28° 45' 36.8" N	19° 49' 33.9" N
Longitude	78° 57' 51" E	72° 46' 47.47" E	17° 52' 56.6" W	155° 8' 19.9" W
Altitude (m)	4500	1680	2324	4207
Aperture (m)	2	1.2	2.5	3
Camera	NIR Imager	NICMOS III	NOTCAM	SPeX
Frame Size	512 × 512	256 × 256	1024 × 1024	1024 × 1024
Pixel Scale	0.21"	0.5"	0.08"	0.12"
Local Time	UT + 5:30	UT + 5: 30	UT - 1:00	UT - 10:00
Observation Dates in May 2004	May 4-11	May 4-7	May 3-6	May 4-8
Observation Dates in July 2004	July 4-11	N/A	None due to weather	July 4-13

The apparent size of the disk of Venus increased from about 27.2" to about 43.1" from May 3 to May 11th as inferior conjunction approached (June 8, 2004) and decreased from 43" to 27" during July 3 – 11 after the conjunction. Observations were made by one of the investigators at each site with the help of the local support staff. HCT observations were obtained remotely at CREST with the help of a support astronomer at the remote control site (Hosakote) and telescope operators at Hanle. Star calibration observations were obtained at the end of the Venus observations in order to maximize the observation times for Venus. Dark and sky flats were obtained on most of the nights from all sites.

At HCT, the shutter was partially closed to reduce to approximately 1m to decrease the amount of light to prevent detector saturation. A stuck filter wheel (NOT) impacted collection of data at multiple wavelengths; otherwise the observations were acquired without much difficulty. Passing clouds occasionally necessitated adjustments in exposure

times at HCT and Mt. Abu. The partially closed shutter at HCT unfortunately affected the image quality somewhat as discovered later during examination of calibration star images. Since the focus of the current investigation is to measure cloud motions, the stuck filter wheel at NOT did not have any impact.

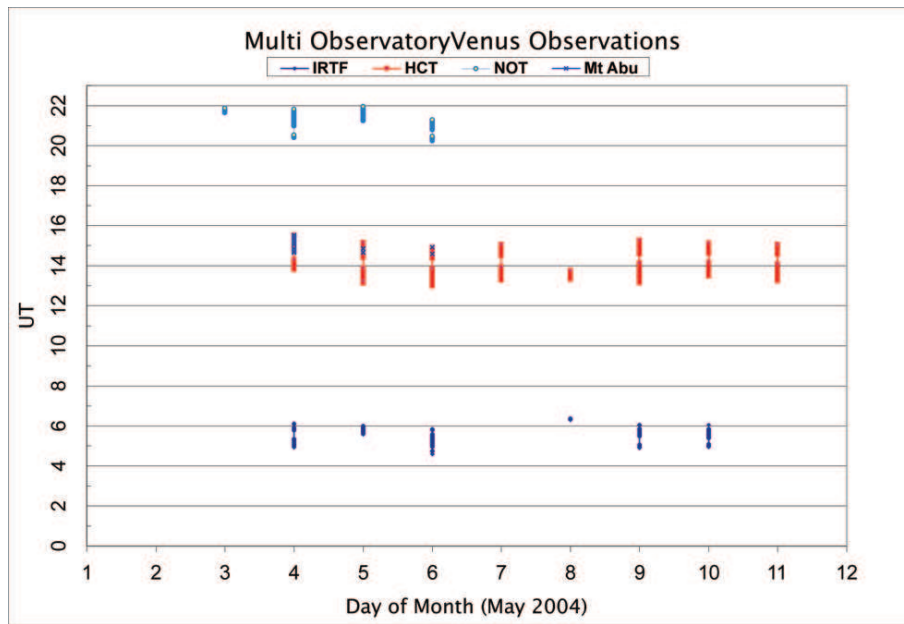


Figure 1. Temporal coverage of the observations in May 2004.

Figure 1 summarizes the observations collected from HCT, Mt. Abu, NOT and IRTF. Shown in the figure are the times of day (UT) when each location was able to acquire observations. Uncooperative sky conditions prevented observations at Mt. Abu Telescope after May 6. Weather on May 8 was not conducive to extended observations at IRTF, NOT also. Only HCT was able to obtain data consistently over the campaign duration. Sample images from each of the sites on May 4 are shown in Figure 2. For comparison, an image acquired by an amateur astronomer in UV is also included to show the extent of the sun-lit crescent of Venus which appears dark due to saturation in the near-infrared images.

Table 2 provides the Earth Venus observing geometry as computed by the Jet Propulsion Laboratory's Horizons On-Line Ephemeris System¹ over the duration of the campaign.

¹Solar System Dynamics Group, Jet Propulsion Laboratory, 4800 Oak Grove, Pasadena, CA 91109 USA. URL – <http://ssd.jpl.nasa.gov/>

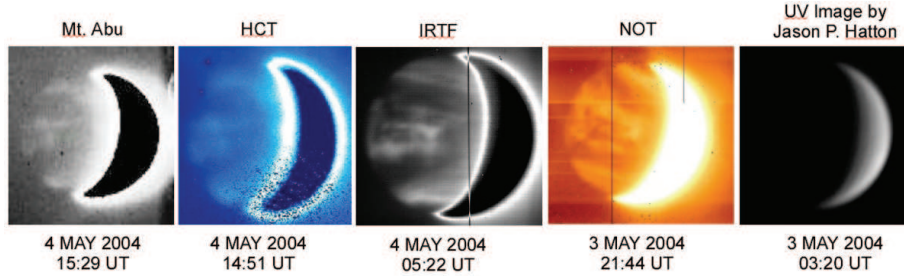


Figure 2. Sample images from IRTF, HCT, Mt. Abu and NOT acquired on May 4 2004. For comparison, a UV image obtained on May 3 by an amateur astronomer is also shown on the right.

Table 2. Venus observing geometry.

Date	Apparent Magnitude	Angular Diameter (arcsec)	Sub-Earth Longitude	Sub-Earth Latitude	Phase Angle (degrees)
3-May-04	-4.51	37.25	285.27	-5.35	117.1433
4-May-04	-4.51	37.84	287.23	-5.33	118.2777
5-May-04	-4.51	38.45	289.16	-5.30	119.4384
6-May-04	-4.51	39.07	291.06	-5.27	120.6266
7-May-04	-4.51	39.70	292.94	-5.24	121.8431
8-May-04	-4.50	40.35	294.78	-5.20	123.0888
9-May-04	-4.50	41.01	296.59	-5.15	124.3648
10-May-04	-4.50	41.67	298.38	-5.10	125.6721
11-May-04	-4.49	42.35	300.13	-5.04	127.0116
3-Jul-04	-4.44	44.92	3.06	3.35	132.4999
4-Jul-04	-4.44	44.21	4.67	3.42	131.0481
5-Jul-04	-4.45	43.51	6.32	3.48	129.6328
6-Jul-04	-4.46	42.81	8.00	3.54	128.2528
7-Jul-04	-4.46	42.13	9.72	3.59	126.9073
8-Jul-04	-4.47	41.45	11.47	3.64	125.5951
9-Jul-04	-4.47	40.79	13.25	3.68	124.3153
10-Jul-04	-4.48	40.14	15.06	3.71	123.0666
11-Jul-04	-4.48	39.50	16.90	3.74	121.8480

3. Processing and measurement of feature motions

Images were processed to remove bias and pixel to pixel variations by using the dark noise and flat field images acquired at each site on each day. The images were navigated by determining the planet image center using a limb fit to the non-crescent portion of

the Venus disk with a circle of the anticipated pixel size. In the absence of star images in the same frame, deconvolution was not performed to improve the quality of images from any site. The IRTF data, with a much higher pixel scale, produced the best spatially resolved data.

The image orientation was verified using the cusp locations. The sub-earth and sub-solar latitudes were computed for the image using the JPL/NAIF Toolkit library (Acton, 1999). Animations of all of the acquired images from each site on each day were inspected to look for any spurious features due to internal reflections in the telescope optics that might be misinterpreted as features on the Venus disk, but none were found that impacted feature tracking. This also allowed a quick selection of the best images to stack and to improve the signal to noise ratio, although for the purpose of tracking it was not essential.

Figure 3 shows two examples of HCT images with overlaid latitude-longitude grids that illustrate the variety and variability of atmospheric features seen at near infrared wavelengths. In Figure 3b, the features are qualitatively similar to those seen at ultraviolet wavelengths, whereas in Figure 3a, the features appear quite different. Navigated images were re-mapped in a rectilinear $0.5 \times 0.5^\circ$ latitude longitude map and displayed as a time lapse sequence to make visual identifications in order to measure the displacements using procedures that have been used previously (Sromovsky et al., 1995; Limaye et al., 1991).

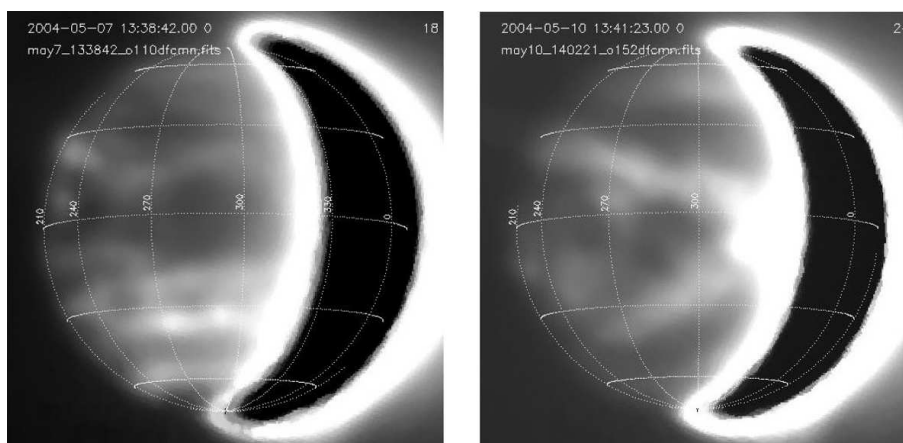


Figure 3. Venus night-side emission images from HCT with overlay planetary latitude-longitude grids obtained on May 7th 13:38:42 UT (a, left) and on May 10 (b, right, 13:41:23 UT).

Atmospheric feature motions were measured by three analysts independently using simple visual tracking in both mapped and unmapped sequences. As an example Figure 4 shows a plot of measured featured longitudes as a function of time of the image in which the feature was located. A linear regression fit to such measurements provided the longitudinal (zonal or east-west) and the latitudinal positions yield the meridional

(north-south) component of the feature motion. The linear fit assumes fixed drift rate for the features over the interval spanning the first and the last image in which the feature locations are measured. As the atmospheric features are known to be quite dynamic on Venus, the size of the feature dictates the period over which this assumption is valid, with the largest features in $2.3 \mu\text{m}$ images lasting almost a week or longer.

Generally “bright” or higher radiance features were tracked, although occasionally “dark” or lower radiance features, when visible as isolated features, were also tracked. The bright areas represent low opacity in Venus’s lower cloud deck, which pass thermal radiation from the surface and lower two scale heights of the atmosphere. Dark regions are presumably silhouettes of clouds in the lower and middle cloud decks. No consistent differences can be discerned between the drift rates of dark and light features. The vertical variation of the east-west flow has been observed from entry probes previously and known to be variable with location on the planet, and possibly time, although the general characteristics are consistent.

Cross correlation techniques were not used for feature tracking given the significant differences in the resolution of the original data from the multiple observatories leading to vast differences in the spatial detail visible in the images.

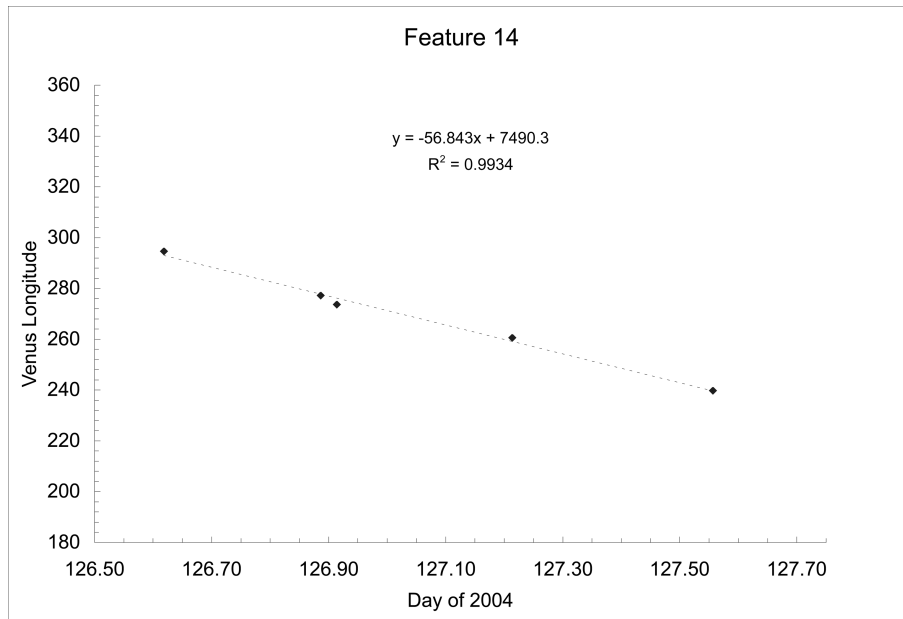


Figure 4. An example of feature movement in longitude on Venus. The linear regression fit provides a measure of the drift rate (-56.84 degrees/day, or 66.5 ms^{-1} for an assumed altitude of 48 km above the mean surface from east to west) for the feature over the duration and a measure of the confidence (regression coefficient).

4. Results

Tracking by three individuals resulted in ~ 100 cloud motion vectors, with 11 from features located in pairs of images and 2 from measured locations in as many as 11 images, with most vectors resulting from feature locations in four or five images.

Table 3 lists the results obtained by averaging the tracking results in 10-degree wide latitude bins. The results for the meridional flow (V) are presented only for the sake of completeness. The zonal flow profile with latitude is shown in Figure 5, which suggests that there is some asymmetry across the two hemispheres, with the southern hemisphere generally showing faster east-west flow (U) than the northern hemisphere. The reasons for such an asymmetry are unknown and not at all expected, either from theoretical expectations or prior measurements. Previous measurements (Crisp et al., 1991; Carlson et al., 1991) do show two distinct flow regimes, so perhaps our results are an indication of such a situation. However, we have limited data at this point to make any definitive statements.

The standard deviation of the zonal component (RMS U) varies with latitude and reflects both measurement errors and very likely real variability of the atmosphere. The measurement errors are likely to be larger in the -32.5° and $+41^\circ$ latitude bins than in the $\pm 25^\circ$ latitude bins due to the difficulty in identifying features as reflected by the general fall off in the number of useful features to track with latitude such that the RMS values also reflect fewer statistics. The RMS values for the most poleward bins are just marginally greater than the RMS for the equatorial bin, but the number of features tracked at high latitudes is much smaller.

Table 3. 10-degree latitude average profile of the zonal component of the drift of 2.3 micron atmospheric features on Venus.

Avg. Lat.	U (m/s)	RMS U (m/s)	V (m/s)	RMS V (m/s)	Number of vectors/bin	Speed (m/s)	Period (days)
-58.67	-58.58		5.47		1	58.6	7.6
-32.5	-57.5	7.0	-0.98	6.06	4	57.5	7.7
-25.5	-58.4	19.7	-1.46	6.79	9	58.4	7.6
-22.0	-61.8	14.7	-4.40	3.72	3	61.8	7.2
-14.6	-62.5	11.7	-7.88	13.13	12	62.5	7.1
-12.3	-61.6	12.2	-7.96	15.32	7	61.6	7.2
-3.7	-62.2	7.0	-1.19	6.07	11	62.2	7.1
2.3	-46.1	4.1	-9.47	3.60	6	46.1	9.6
14.2	-44.6	10.5	-1.54	10.91	15	44.6	10.0
23.8	-40.0	19.6	-2.18	3.94	6	40.0	11.1
41.0	-27.3	6.3	-7.1	6.3	2	27.3	16.3

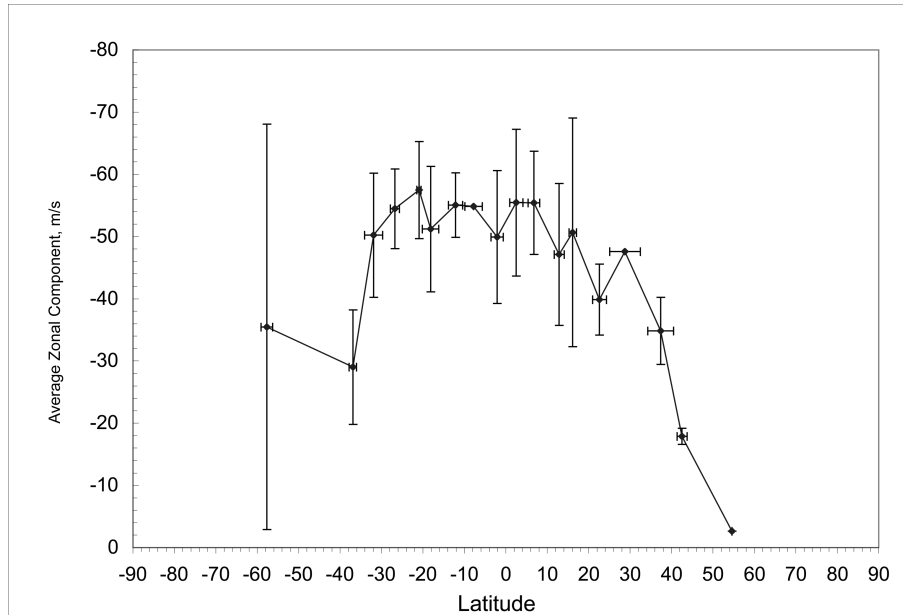


Figure 5. Latitudinal profile of the east-west component of motion of the $2.3 \mu\text{m}$ atmospheric features generated by binning the measured vectors in 10-degree wide bands. The error bars show the root mean square deviation for each bin, for both the latitude and the zonal component.

Limited spatial resolution of the data and the small magnitude of the north-south flow in the atmosphere of Venus precludes any useful measurements with confidence. Given the RMS deviation it is difficult to put any confidence even in the general direction of the flow (poleward or equatorward), a prime unknown for Venus on a global scale. It is known from entry probe measurements that both poleward and equatorward motions are found in the deep atmosphere of Venus, but these observations span a period of many years and are too sporadic. In view of the poleward flow observed on Venus from tracking of ultraviolet cloud features (~ 65 km altitude), from mass continuity and numerical models, large scale equatorward flow at some depths in the Venus atmosphere is expected, and measuring it with confidence remains an unrealized objective due to observing difficulties and its small magnitude.

The atmospheric rotation rates indicated by the measurements, from $\sim 7 - 16$ days are consistent with previous observations of cloud motions from entry probes as well as from analysis of fly-by and orbiter images. (Limaye et al., 1988; Schubert, 1983).

Finally, feature motion results obtained from July 2004 IRTF observations alone indicate an average zonal flow profile with latitude that is somewhat different from the results presented here. These IRTF observations have much higher spatial resolution (0.5 arc-sec/pixel) and the tracking was performed with observations taken each day. Preliminary

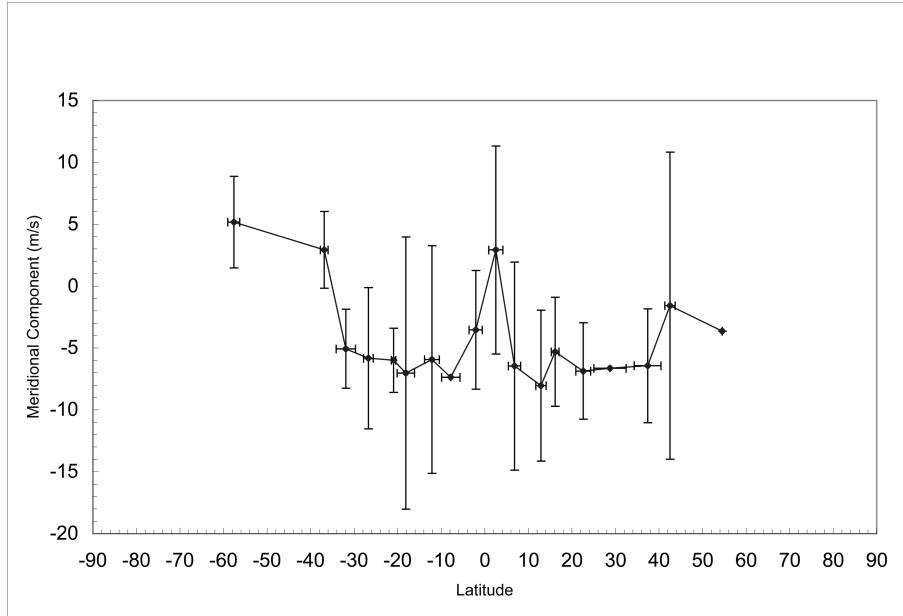


Figure 6. Latitudinal profile of the north-south (meridional) component of motion of the 2.3 μm atmospheric features generated by binning the measured vectors in ~ 10 -degree wide bands. The error bars show the root mean square deviation for each bin, for both the latitude and the zonal component.

results indicate that the east-west flow may be as strong as $\sim 75 \text{ ms}^{-1}$ at 40°N and 40°S latitudes. Although the difference with the results presented here could be due to the fact that we are limited (due to lower spatial resolution) to tracking large features lasting longer compared to smaller features tracked from the July 2004 observations (Tavenner et al., 2005), the difference is also likely indicative of the dynamic state of the lower atmosphere, whose driving mechanisms are still a puzzle.

The Venus Express spacecraft will arrive at Venus in April 2006 and will commence sending data shortly after it is inserted into orbit around Venus. In October 2007, NASA's MESSENGER spacecraft on its way to orbit Mercury will approach Venus from the day side and fly past, providing high spatial and temporal observations of Venus from which the details of the Venus global atmospheric circulation can be obtained. Limited spacecraft communication resources and instrument point issues limit the amount of data from imaging instruments that can be obtained, and careful planning to maximize the science return is essential. Studies such as this one provide us with valuable information to plan the observations from these missions. Thus, groundbased observations of Venus at near infrared wavelengths with continuously improving instruments are particularly needed now to plan better for the observations from these missions and in the interpretation of the data, both collected in the past and future.

Acknowledgements

It is a pleasure to acknowledge the support from the staff of Mt. Abu (Mr. Rajesh Shah), Hanle, NOT and the IRTF observatories. We are grateful to the hospitality and support provided by the staff of the Physical Research Laboratory which operates the Mt. Abu Telescope and also the staff of CREST/Indian Institute of Astrophysics for enabling observations from HCT. These observations would not have been possible without the interest and support of Dr. Tushar Prabhu (IIA), Dr. B.G. Anandarao and Dr. Chandrasekhar (Physical Research Laboratory) and G. Emerson. Mt. Abu and Himalayan Chandra Telescope are supported by grants from the Department of Science and Technology, and the Indian Space Research Organization, Govt. of India.

The results presented here are also based on observations made with the Nordic Optical Telescope, operated on the island of La Palma jointly by Denmark, Finland, Iceland, Norway, and Sweden, in the Spanish Observatorio del Roque de los Muchachos of the Instituto de Astrofísica de Canarias. We also acknowledge the support provided by the Visiting Astronomer at the Infrared Telescope Facility, which is operated by the University of Hawaii under Cooperative Agreement no. NCC 5-538 with the National Aeronautics and Space Administration, Office of Space Science, Planetary Astronomy Program, and the Swedish National Space Board as well as the Swedish Research Council for providing research funding and travel grants.

Finally, comments by an anonymous referee were useful in improving this manuscript and those efforts are gratefully acknowledged.

References

- Acton, C.A., 1999, in *Proceedings 30th Annual Lunar and Planetary Science Conference*, March 15-29, 1999, Houston, TX, *Abstract no.* 1233.
- Allen, D.A., 1987, *Icarus*, **69**, 221.
- Allen, D. A., and Crawford, J.W., 1984, *Nature*, **307**, 222.
- Baines, K.H., and Carlson, R.W., 1991, *Bull. Amer. Astr. Soc.*, **23**, 1195.
- Bell, J., et al., 1991, *Science*, **252**, 1293.
- Bezard, B.C., DeBergh, Crisp, D. and Maillard, J.-P., 1990, *Nature*, **345**, 508.
- Carlson, R.W. et al., 1991, *Science*, **253**, 1541.
- Carlson, R.W., Kamp, L.W., Baines, K.H., Pollack, J.B., Grinspoon, D.H., Encrenaz, Th., Drossart, P., and Taylor, F.W., 1993, *Planet. Space Sci.*, **41**, 477.
- Chanover, N. J., Glenar, D. A. D, and Hillman J.J., 1998, *J. Geophys. Res.*, **103**, 31335.
- Chicarro, A.F., 2003, Europe goes to Mars and Venus, *Lunar and Planetary Institute Conference Abstracts*.
- Crisp, D. S., McMudroch, K., Stephens, W.M., Sinton, B., Ragent, K. W., Hodapp, R.G., Probst, L.R., Doyle, D.A., Allen J. Elias, 1991, *Science*, **253**, 1538.
- Kerzhanovich, V.V., and Limaye, S.S., 1985, *Adv. Space Res.*, **5**, No. 11, 59.
- Limaye, S.S., and Sromovsky, L.A., 1991, *J. Geophys. Res.*, **96**, 18, 941.
- Limaye, S.S., Grassotti, C., and Kuetemeyer, M.J., 1988, *Icarus*, **73**, 193.

- Meadows, V.S., and Crisp, D., 1996, *J. Geophys. Res.*, **101**, 4595.
- Rayner, J.T., Toomey, D. W., Onaka, P. M., Denault, A. J., Stahlberger, W. E., Vacca, W. D., Cushing, M. C., and Wang, S., 2003, *PASP*, **115**, 362.
- Schubert, G., 1983, in *Venus*, (Ed. D. M. Hunten, *et al.*), University of Arizona Press, Tucson, Arizona, Chapter 21.
- Sromovsky, L.A., Limaye, S.S., and Fry, P.M., 1995, *Icarus*, **118**, 25.
- Svedhem, H., Titov, D., McCoy, D., Rodriguez-Canabal, J., and Fabrega, J., 2005, *American Geophysical Union Fall Meeting Abstract no. P23E-01*.
- Tavener, T., Young, E.F., Murphy, J., Bullock, M. A., Coyote, S., Rafkin, S., 2005, *Bull. Amer. Astr. Soc.*, **37**, 742.